

PACS photometer calibration block analysis

Moór, A. · Müller, Th. G. · Kiss, Cs. ·
Balog, Z. · Billot, N. · Marton, G.

Received: date / Accepted: date

Abstract The absolute stability of the PACS bolometer response over the entire mission lifetime without applying any corrections is about 0.5% (standard deviation) or about 8% peak-to-peak. This fantastic stability allows us to calibrate all scientific measurements by a fixed and time-independent response file, without using any information from the PACS internal calibration sources. However, the analysis of calibration block observations revealed clear correlations of the internal source signals with the evaporator temperature and a signal drift during the first half hour after the cooler recycling. These effects are small, but can be seen in repeated measurements of standard stars. From our analysis we established corrections for both effects which push the stability of the PACS bolometer response to about 0.2% (stdev) or 2% in the blue, 3% in the green and 5% in the red channel (peak-to-peak). After both corrections we still see a correlation of the signals with PACS FPU temperatures, possibly caused by parasitic heat influences via the Kevlar wires which connect the bolometers with the PACS Focal Plane Unit. No aging effect or degradation of the photometric system during the mission lifetime has been found.

A. Moór
Konkoly Observatory, MTA CSFK
Tel.: +36-1-3919341
Fax: +36-1-2754668
E-mail: moor@konkoly.hu

Th. Müller
Max-Planck-Institut für extraterrestrische Physik, Garching, Germany

Cs. Kiss and G. Marton
Konkoly Observatory, MTA CSFK

Z. Balog
Max-Planck-Institut für Astronomie, Heidelberg, Germany

N. Billot
Instituto de Radio Astronomía Milimétrica, Granada, Spain

Keywords PACS bolometers · calibration block observations · long term behaviour of bolometers

1 Introduction

During the nearly four-year long mission of the *Herschel Space Observatory* (Pilbratt et al., 2010) more than 21000 photometric observations were performed with the Photoconductor Array Camera & Spectrometer (PACS, Poglitsch et al., 2010) onboard the spacecraft. PACS photometric observations were performed by two bolometer arrays that operate parallel acquiring images at 70 or 100 μm (blue array) and at 160 μm (red array). These observations, by their nature, were heterogeneous in terms of different characteristics, including the utilized observing mode, brightness of the target and the sky background, the duration of the measurement. However, each PACS photometric observation includes at least one calibration block (CB) measurement that consists of chopped observations between the two PACS internal calibration sources (CSs). CB observations – on the contrary to science measurements – are always performed using a standard, identical manner. Thus, they constitute a homogeneous data set that enables the monitoring of the number of dead, bad/noisy or saturated pixels and particularly the possible short- and long-term evolution of bolometer response during the full mission lifetime on the basis of a well-defined differential signal from the PACS calibration sources. Calibration blocks are also very useful to verify changes on a given operational day (OD, day elapsed since the launch of the spacecraft) or a sequence of ODs for science projects with repeated measurements of the same source in a short period of time.

In order to investigate the behaviour of the bolometer responsivity, we compiled a database of photometer calibration block observations by processing all PACS photometric measurements, including those obtained in SPIRE/PACS parallel mode. Using this database we searched for the dependencies of detector signal output on various instrument and satellite parameters. A preliminary analysis of the CB signals and the features observed in the first year of the *Herschel* mission are summarized in Billot et al. (2010).

2 Calibration block observations and data processing strategy

2.1 Internal calibration sources

For the continuous monitoring of the detector noise and responsivity we need a source of constant flux that is provided by the internal calibrators within the PACS instrument. The two grey body calibration sources are placed near the entrance to the instrument (Fig. 1 left), outside of the Lyot stop, to have approximately the same light path for observation and internal calibration. They provide far-infrared radiation loads slightly below (CS1, 48 Ω , 55 K)

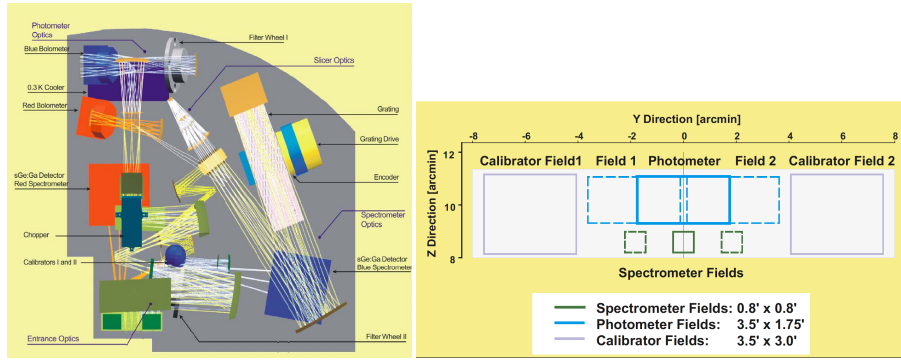


Fig. 1 Left: Optical layout of PACS. Calibration sources are placed at the entrance of the instrument. Right: The PACS field-of-view in combination with the chopper positions of the optical axis and the positions on both PACS calibration sources (CSs). In the PHOT calibration block chopping between the two CSs is performed. Both figures are taken from the PACS Observer’s Manual.

and above (CS2, 58 Ω , 60 K) the telescope background at around $100\mu\text{m}$ (both loads are below the telescope background at the shortest wavelengths and above at the longest wavelengths due to differences between the telescope and calibration sources emissivities). They uniformly illuminate both the field of view and the Lyot stop, to mimic the illumination by the telescope.

Details about the calibration sources are specified in the “Herschel PACS Calibration Source Interface Control Document” (PACS-KT-ID-007, Issue 4, Kayser-Threde GmbH, April 2004). At typical operation temperatures each source has an average power of well below 1.6 mW, at heating up phases a peak power of 10 mW can be applied, resulting in maximum currents of up to 11 mA at the lower temperature range and about 7 mA at 100 K.

The heater sensor control electronics guarantees a stability of better than 5 mK that corresponds to $< 5 \text{ m}\Omega$ at 50 K, requiring a 15 bit resolution for the specified temperature range.

The output load of the calibration sources was calibrated during instrument level tests against two highly stable and well characterised black bodies inside the PACS optical ground segment equipment (OGSE black bodies). The observed resistance values (see Fig. 2) are $48.0004 \pm 0.0015 \Omega$ (13 m Ω peak-to-peak) for CS1 and $58.0000 \pm 0.0019 \Omega$ (14 m Ω peak-to-peak) for CS2. The m Ω variations can be easily translated into mK temperature variations via the calibration certificate (chapter 31 of the cryogenic qualification model Kaiser-Threde GmbH end-item data package): A 20 m Ω resistance variation corresponds roughly to a 10 mK temperature variation (in the 55 to 60 K range) which is about 0.05 per cent in flux or surface brightness, well below the bolometer measurement accuracy. Our extracted peak-to-peak resistance values are well within the assumed 20 m Ω . As expected from these calculations, we found no correlation between the residual fluctuations (seen after all corrections have been applied) and the measured calibration source resistance values.

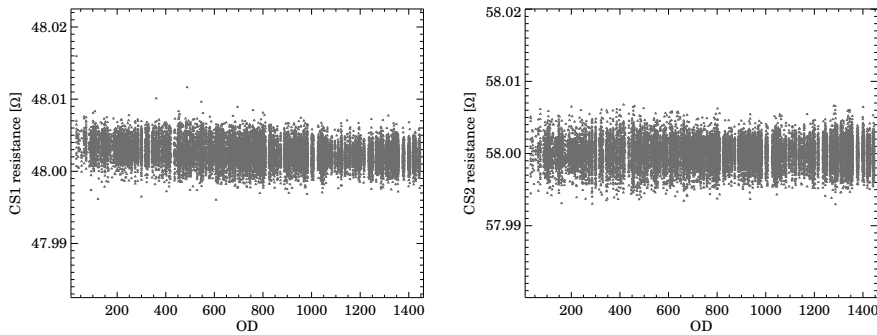


Fig. 2 CS1 (left) and CS2 (right) resistance values as a function of OD.

2.2 Design of calibration block observations

A calibration block observation contains several chopper cycles on both PACS calibration sources (Fig. 1 right). The chopper moves with a frequency of 0.625 Hz between the two PACS CSs. In total 19 chopper cycles are executed within a given measurement, each chopper plateau lasts for 0.8 s producing 8 frames in the down-link (4 bolometer readouts are averaged), hence a CB observation lasts for about 30 s in total. In the SPIRE/PACS parallel mode the setting for blue array CB measurements is slightly different since 8 bolometer readouts are averaged in the blue channel, in the red channel 4 readouts are averaged exactly as in the PACS prime mode.

A typical PACS photometer measurement contains one calibration block observation, that precedes the science part of the measurement in the observational sequence. However, there are some observations for which more than one CB measurements were obtained, e.g. in the case of SPIRE/PACS parallel mode observations the science block are typically bracketed by two CBs. Calibration blocks are executed exactly in the same filter, gain and SPU setting as the science block that they belong to. CBs are performed in the target acquisition phase. Up to the OD545 the calibration block was always executed towards the end of the target acquisition phase (slew) and the science part was separated from the calibration block by only 5 s delay time. However, because the bolometer signals display a noticeable drift after the calibration block for about 30 s this strategy was revised and after OD546 the CBs were executed at the earliest possible moment during the slew allowing in many cases for a longer signal stabilisation before the science observation started.

Due to their design, calibration blocks can provide a clean start for the subsequent science observations and allow the determination of bolometer response using the derived differential signal of PACS calibration sources.

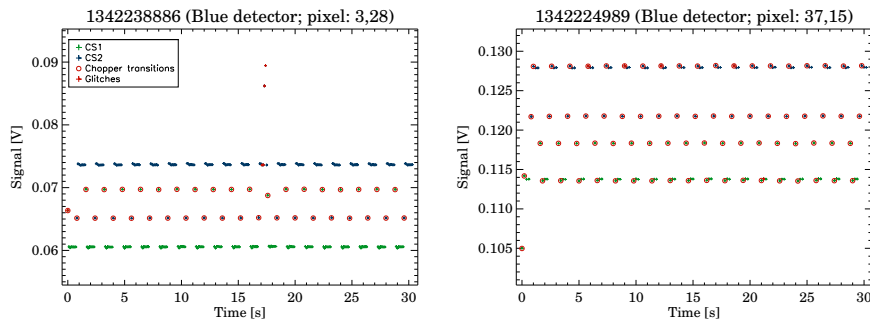


Fig. 3 Data stream in a typical calibration block observation obtained with the blue detector in the PACS prime mode (left) and in the PACS parallel mode (right). The two CS signals were derived from the cleaned chopper plateaus.

2.3 Data processing of CB observations

Our CB processing scheme includes the following steps: 1) identify the calibration block(s) within the specific measurement (perform *detectCalibrationBlock* and *findBlocks*, then select data points that belong to the CB); 2) perform basic data processing steps (*photFlagBadPixels*, *photFlagSaturation*, *photConvDigit2Volts*, *photMMTDeglitching*); 3) after eliminating chopper transitions (the first point in each chopper plateau for PACS prime observations and for PACS parallel observations with red detector, the first two points in the case of blue parallel CBs) and glitches, determine the CS1 and CS2 signal levels for each pixel ($S_{CS1}^{i,j}$, $S_{CS2}^{i,j}$, where i and j are the i^{th} and j^{th} pixels of the blue or red array) by computing an outlier-resistant average of chopper plateaus¹. Then differential signals are determined as $S_{diff}^{i,j} = S_{CS2}^{i,j} - S_{CS1}^{i,j}$ for each detector pixel. Figure 3 displays the signal in a typical calibration block observation.

As a final step we 1) calculate robustly averaged CS1, CS2 and differential signals for the blue and red array using all unmasked pixels, and 2) extract additional relevant parameters from the measurement and the related house-keeping data that are necessary for the trend analysis (e.g. the FineTime of the observation, evaporator temperature, etc.).

2.4 Database of CB observations

Altogether 20795 PACS photometric (including 854 SPIRE/PACS parallel) observations are available in the Herschel archive. This number includes both scientific and calibration observations. We processed all CBs that belong to these measurements. Although most observations include only one CB measurement, science and calibration observations in early mission phases (up to

¹ Applying IDL's *biweight_mean* routine that uses Tukey's biweight method for robust moment estimation.

OD150) were performed with more than one (up to 18) CBs. SPIRE/PACS parallel mode observations typically contain two CBs. Therefore our final database contains 22000 calibration block observations in total.

3 Results

The actual bolometer response is well characterized by the differential signal of the two internal calibration sources measured in the corresponding CB observation. By investigating the evolution of differential CS signals throughout the *Herschel* mission we can study the long term behaviour of the bolometer response. As a first step of this study we searched for possible systematic trends between differential signals and instrumental parameters. Then we developed corrections to the revealed trends and applied them to our data. Finally we used the corrected differential signals to study the long term variations of bolometer response.

We found that S_{diff} correlates well both with the evaporator temperature and the temperature of the focal plane unit. Moreover, signal levels also show a short drift in the first 0.5 h after the cooler recycling has finished.

3.1 Correlation with evaporator temperature

During the mission a ^3He cooler was used to ensure sub-Kelvin temperature for the operation of PACS photometer. The evaporation of ^3He provides a very stable temperature environment at $\sim 300\text{mK}$. After each cooler recycling procedure, that takes about 2.5 h, there are about 2.5 ODs of PACS photometer observations possible. The evaporator temperature (T_{EV}) rises towards end of cooling cycles (Figure 4).

By investigating the behaviour of S_{diff} as a function of T_{EV} (see Fig. 5) we found a clear correlation between the two parameters for both the blue and the red arrays. The observed trend can be well fitted by a linear relationship enabling a correction for this effect. It is important to note that measured flux densities of standard stars extracted from PACS calibration observations showed very similar trend with evaporator temperature and their photometry can be improved by applying our pixel-based T_{EV} correction for their observations (Balog et al., this issue).

The correlation with T_{EV} is very clear, but the related corrections are typically well below 1%, however, they vary slightly from pixel-to-pixel. It is only $\sim 1.2\%$ of all measurements for which this correction is larger than 1%!

3.2 Correlation with temperature of focal plane unit

After the T_{EV} correction, we also looked for remaining trends and correlations. We found that differential CS signals also depend on the FPU (Focal Plane Unit) temperature (T_{FPU}). The FPU temperature ("BOL_TEMP_FPU_ST"

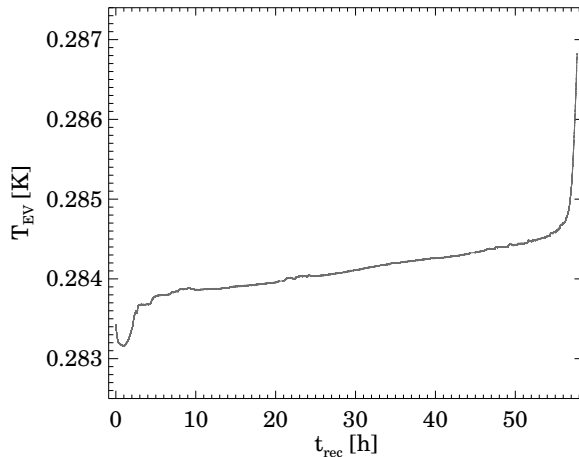


Fig. 4 Variation of evaporator temperature over a given cooler cycle (between OD917 and OD919).

parameter in the housekeeping data) was measured at the 2K structure between two focal planes (Müller, 2009).

The observed trend is not as strong as in the case of T_{EV} but can also be fitted by a linear relationship (Figure 6). Interestingly, the red array is not affected by this phenomenon. Though the reason behind the observed trend has not been completely understood yet, it might be that the heat load of the FPU structure influences the bolometers via the Kevlar wires which connect the 300 mK bolometers to the 2K FPU structure. The variation of FPU temperature may affect calibration blocks only and may not cause changes in the science observations.

3.3 Drifting effect at early recycling times

As Figure 7 demonstrates, differential CS signals also depend on the time elapsed since the end of the last cooling recycling procedure (t_{rec}). At the very beginning of PACS observing sessions a stabilization effect can be recognized. This drift is only a very small effect and is only seen during the first ~ 30 minutes after the recycling has finished. In most cases this drift may usually be covered in the initial slew to the first science target after the recycling. The observed trend can be well fitted by a simple model:

$$S_{diff}^{i,j} = a_0^{i,j} \exp(-t_{rec}/a_1^{i,j}) + a_2^{i,j},$$

where $a_0^{i,j}$, $a_1^{i,j}$, and $a_2^{i,j}$ are parameters to be fitted.

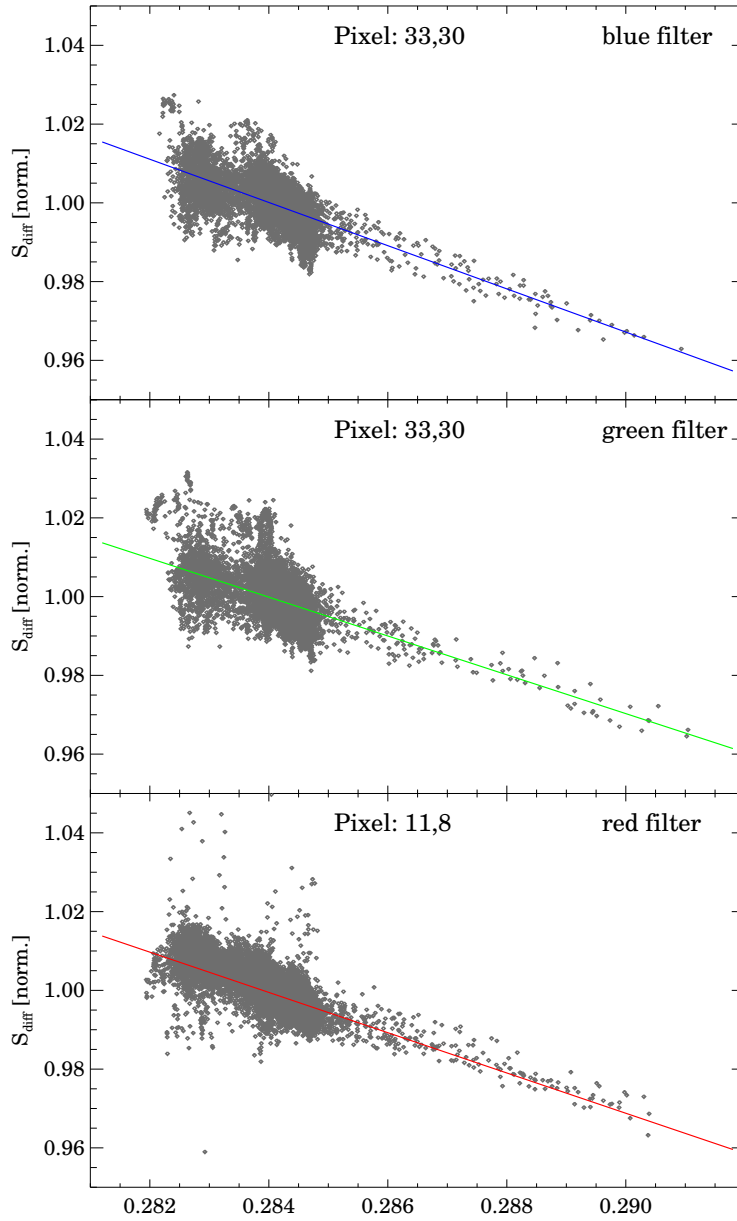


Fig. 5 Normalized differential CB signals of a selected pixel as a function of evaporator temperature for measurements executed with blue (at $70\mu\text{m}$, upper panel), green (at $100\mu\text{m}$, mid panel), and red (at $160\mu\text{m}$, lower panel) filter. The observed trend can be well fitted by a linear (displayed as blue, green, and red lines).

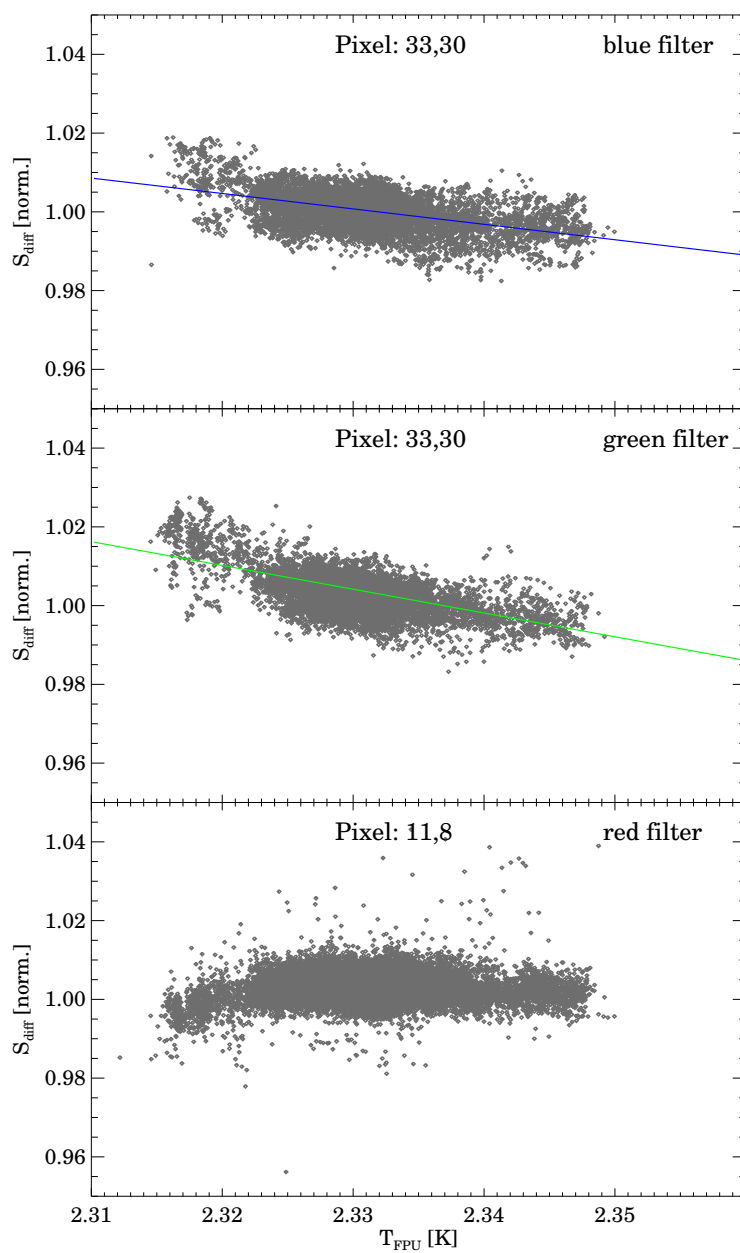


Fig. 6 Normalized differential CB signals for a selected pixel as a function of FPU temperature (for blue, green, and red filter observations). The plotted CB signals have already been corrected for T_{EV} effect. The observed trend can be well fitted by a linear (displayed as blue and green lines).

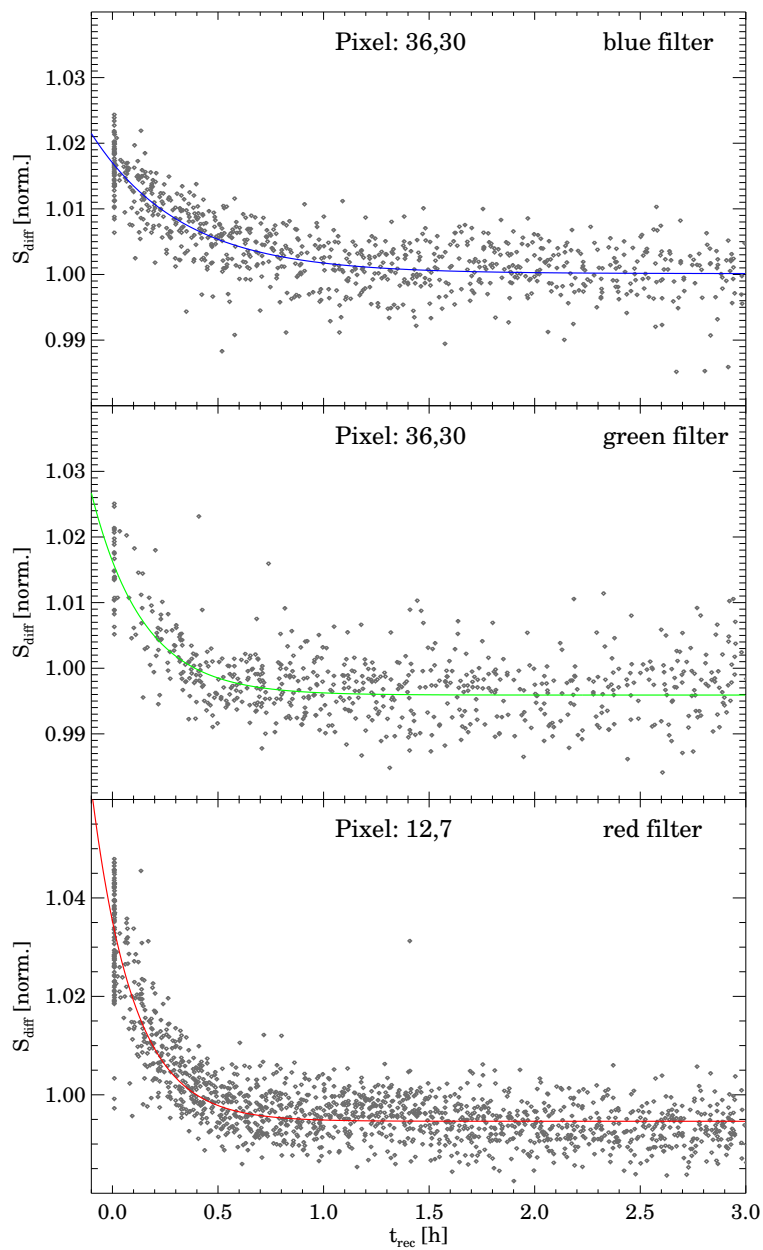


Fig. 7 Normalized differential CB signals for a selected pixel as a function of recycling time (for blue, green, and red filter observations). The plotted CB signals have already been corrected for T_{EV} effect. Model fits are shown as blue, green and red lines.

3.4 Evolution of differential CB signals

As Figure 8 shows, the level of differential signals and thus the PACS bolometer response was stable over the entire mission lifetime. The stability of the

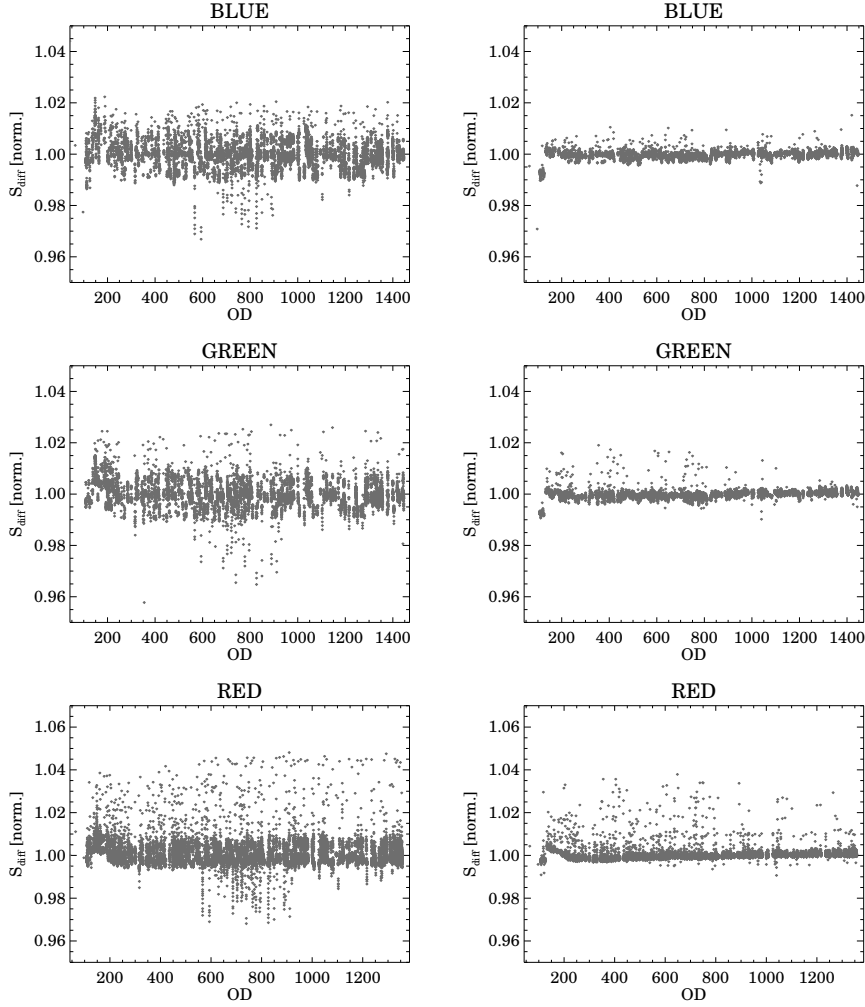


Fig. 8 Left panels: Averaged differential CS signals as a function of operational day without any correction for blue (upper panel), green (mid panel), and red filter (lower panel) CB measurements. Right panels: Averaged differential CS signals as a function of operational day after corrections for T_{EV} , T_{FPU} and t_{rec} were applied. The red PACS detector consisted of 2 bolometer matrices (matrix 9 and matrix 10). After OD1375 one of the two red channel subarrays (matrix 9) was affected by a serious anomaly. Therefore red data were not plotted for OD > 1375.

differential CS signal even without any correction was less than $\sim 0.5\%$ (stan-

standard deviation) or $\sim 8\%$ (peak-to-peak) in blue/green/red observations (Fig. 8, left panels or in Table 1). By applying all of our corrections we can achieve a stability level of $\sim 0.12\%$ for blue array observations and 0.2% (standard deviation) for data obtained using the red bolometer (Fig. 8, right panels). The peak-to-peak variation of the final data set is lower than 2, 3 and 5% in blue/green/red CB observations. As Table 1 shows the correction related to T_{EV} is by far the most important among all corrections we applied. Due to

Table 1 Influence of corrections on the standard deviation of differential CS signals

Processing stage	Standard deviation of differential CS signals averaged for bolometer arrays [%]		
	Blue filter	Green filter	Red filter
Before corrections were applied	0.49	0.48	0.53
After correction for T_{EV} was applied	0.22	0.22	0.34
After T_{EV} and t_{rec} corrections	0.17	0.16	0.18
After all corrections were applied	0.12	0.13	0.18

this excellent stability the calibration of scientific measurements can be done without using the PACS CBs directly, only the T_{EV} correction – which will be part of future HIPE & pipeline versions – is based on information extracted from the frequent measurements of the PACS internal calibration sources.

The significantly decreased scatter of differential signals allowed us to search for remaining weaker trends in the data set. Our most interesting findings are as follow:

- PACS photometer was operating in dual band mode taking data with a red filter and a blue or green filter simultaneously on two bolometer arrays. We found that the filter of the blue array has an effect on the signal level measured in the red band. As Figure 9 demonstrates, the differential red signals are higher when the $70\mu\text{m}$ filter was placed in the blue channel and lower when the $100\mu\text{m}$ filter was used. This could be caused by slightly different straylight/reflection patterns inside PACS which change with filter wheel positions. Although the difference is very small, a two-sided Kolmogorov-Smirnov test shows that the two distributions are significantly different.
- The red PACS detector is assembled from 2 bolometer matrices. After OD1375 one of the two red channel subarrays (matrix 9) was affected by a serious anomaly and therefore became unusable. As Figure 10 (left) shows the other subarray (matrix 10) remained stable the measured signal level obtained with this part of the detector was not changed after this event.
- All 3 bands show an initial jump/stabilization phase during the first ~ 280 ODs (Figure 10, right). The variation of CB signals is quite similar for all blue array observations (blue/green). The reason of this initial stabilization phase is not understood, but coincides with small variations in the detector setup (orbit prologue) during the early mission phase (see Performance

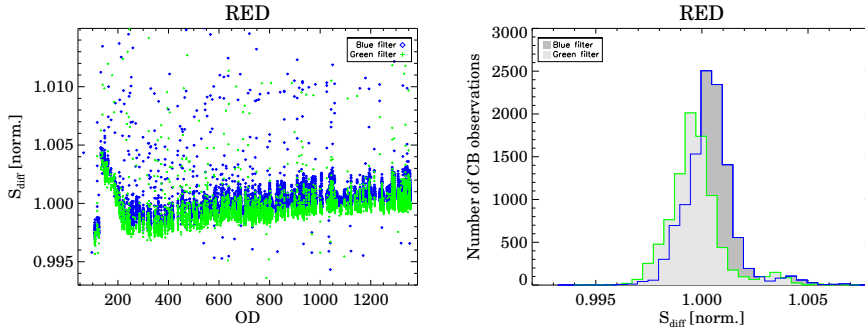


Fig. 9 Left panel: Averaged differential CS signals for the red array as a function of operational day. Red data points obtained with the blue or green short wavelength PACS filter selection are displayed with different symbols. On the right panel we present the distribution of these data.

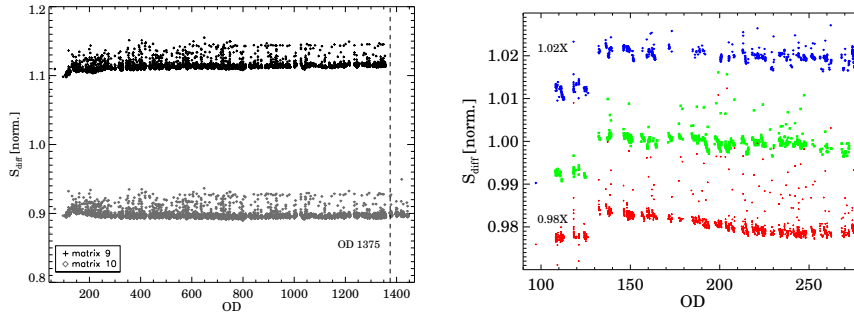


Fig. 10 Left panel: Differential CB signals averaged for the two subarrays of the red detector (matrix 9 and matrix 10) as a function of OD. Right panel: Averaged differential CB signals (for blue, green, and red filter observations) as a function of OD for the early phase of the mission. Note that signals measured with the blue and red filters have been multiplied by a factor of 1.02 and 0.98, respectively, in order to avoid overlapping data points.

Verification Plan, reference below). There is an additional weak trend in the variation of red signals with operational days. After OD 250 the differential CB signals measured in the red band slowly increase with increasing OD (Fig. 9 left). Nielbock et al. (this issue) found similar effects in the chop-nod observations of the fiducial stars that they attribute to a change in the temperature gradient on the primary mirror. Though CSs do not see the primary mirror directly, their signals might be influenced via straylight. We also note that during the commissioning phase of the PACS Photometer the detector bias voltages were modified at OD128 (for more details see Billot et al., 2010). The discontinuity seen in the differential signal levels at around this epoch in Figure 10 (right) might be due to this bias change.

- PACS instrument campaigns – that took about 2.5 ODs – were interrupted by *Daily TeleCommunication Periods* (DTCP) in which the previously collected data were downlinked to Earth. Before OD670 the PACS detector

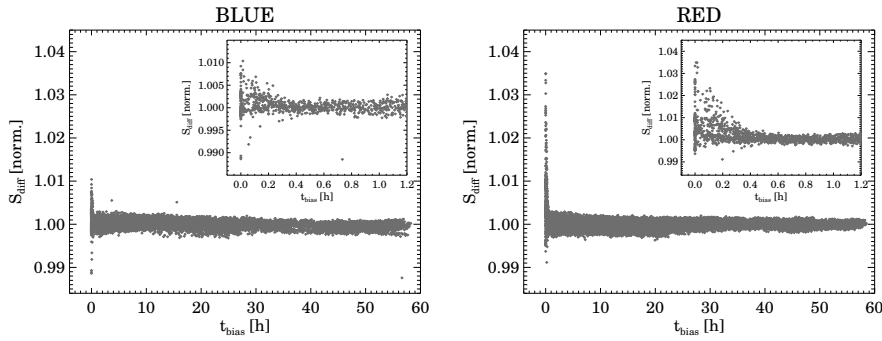


Fig. 11 Averaged differential CB signals for blue and red filter observations as a function of t_{bias} .

was put in safe mode during DTCP and the bolometers were not biased. After that, however, the operational strategy was changed and the PACS bolometers were kept biased during DTCPs. Figure 11 shows the corrected differential CB signals as a function of t_{bias} (the time elapsed since the last biasing of the detectors) for measurements executed with blue (left) and red filter (right), respectively. Observations obtained in the early phase of the mission ($< OD200$) were discarded and not displayed in the figures (in order to avoid early mission stabilization period, as described in the previous paragraph). As these figures demonstrate, most of the remaining outliers are related to observations performed very early after the preceding biasing, implying that these processes are also accompanied by a stabilization effect.

- We note that variation of solar aspect angle has no influence on signal levels.

4 Summary

Using our database of calibration block observations we investigated the long term behaviour of differential CS signals which characterize the evolution of the bolometer response as well. We revealed that variation of evaporator temperature and FPU temperature cause changes in differential signals. Signal levels also show a short drift in the first 0.5h of observing sessions after the cooler recycling. We developed correction methods for all three effects. By applying these corrections the standard deviation of differential CS signals could be decreased significantly. The main cause of differential signal changes is the variation of evaporator temperature. We note that measured flux densities of standard stars show also a similar dependency on T_{EV} . A task that performs this correction will be available in HIPE 12.0. This will improve the photometry for measurements taken either directly after the cooler recycling or very late towards the end of the cooler hold time. The drifting effect observed at low recycling time is more important for the red array than for the blue. The

bolometer response turned out to be very stable over the entire mission lifetime thus the individual calibration blocks do not need to be used in the processing of the corresponding science data. No aging effect or degradation of the photometric system during the mission lifetime has been found.

Acknowledgements We thank our anonymous referee whose comments significantly improved the manuscript. This research has been supported by the PECS programme of the Hungarian Space Office and the European Space Agency (contact number: 98073). CK and AM acknowledge the support of the Hungarian Research Fund (OTKA K-104607) and that of the Bolyai Research Fellowship of the Hungarian Academy of Sciences.

References

1. Balog, Z., Müller, T., Nielbock, M., Altieri, B., Klaas, U., Linz, H., Lutz, D., Moór, A., Billot, N., Sauvage, M., Okomura, K., The *Herschel*-PACS photometer calibration: Point-source flux calibration, *Experimental Astronomy*, this issue (2013)
2. Billot, N., Sauvage, M., Rodriguez, L., et al., CEA bolometer arrays: the first year in space, *SPIE*, 7741, 1 (2010)
3. PACS Performance Verification Phase Plan, Issue 2.0, PICC-MA-PL-001, custodians: Ulrich Klaas & Markus Nielbock
4. Müller, T., Pacs FM (ILT, IST, TVTB, CoP) Full Functional Test: 413 Thermal Behaviour in Photometry, http://pacs.ster.kuleuven.be/Documents/WBS/FlightReports/012/001/tb_phot_v20090703.pdf
5. Nielbock, N., Müller, T., Balog, Z., Klaas, U., Linz, H., The *Herschel* PACS photometer calibration: A time dependent flux calibration for the PACS chopped photometry AOT mode, *Experimental Astronomy*, this issue (2013)
6. Pilbratt, G. L., Riedinger, J. R., Passvogel, T., et al., *Herschel* Space Observatory. An ESA facility for far-infrared and submillimetre astronomy, *A&A*, 518, L1 (2010)
7. Poglitsch, A., Waelkens, C., Geis, N., et al., The *Herschel* Photodetector Array Camera & Spectrometer (PACS): design and in-flight operation and scientific performance, *A&A*, 518, L2 (2010)